



Convenient and Reusable Manganese-Based Nanocatalyst for Amination of Alcohols

Murugan Subaramanian,^[a] Palmurukan M. Ramar,^[a] Ganesan Sivakumar,^[a] Ravishankar G. Kadam,^[b] Martin Petr,^[b] Radek Zboril,^[b] Manoj B. Gawande,^[b] and Ekambaram Balaraman^{*[a]}

The development of new sustainable nanocatalytic systems for green chemical synthesis is a growing area in chemical science. Herein, a reusable heterogeneous *N*-doped graphene-based manganese nanocatalyst (Mn@NrGO) for selective *N*-alkylation of amines with alcohols is described. Mechanistic studies illustrate that the catalytic reaction follows a domino dehydrogenation-condensation-hydrogenation sequence of alcohols

and amines with the formation of water as the sole by-product. The scope of the reaction is extended to the synthesis of pharmaceutically important *N*-alkylated amine intermediates. The heterogeneous nature of the catalyst made it easy to separate for long-term performance, and the recycling study revealed that the catalyst was robust and retained its activity after several recycling experiments.

Introduction

N-alkylated amines are widely employed for the synthesis of various biologically active molecules, agrochemicals, surfactants, and pharmaceutical drugs.^[1] Conventionally, the *N*-alkylation of amines has been achieved by utilizing the corresponding activated derivatives^[2] or by reductive amination of carbonyl compounds.^[3] However, most of these methods require harsh or potentially hazardous reaction conditions and generate stoichiometric waste. The borrowing hydrogenation (BH) deploying simple and abundantly available alcohols as alkylating agents for the C–C or C–N bond-forming reactions has recently received considerable attention.^[4] The formation of water as the only byproduct makes this process environmentally benign and alternative to conventional methods.^[2,5] The BH approach fundamentally comprises several mechanistically distinguished pathways such as dehydrogenation, condensation, and hydrogenation in a single process. It finally yields C–N or C–C bonded compounds with an excellent step- and atom-economy. Thus, the use of widespread alcohol as the alkylating agent for the BH method ensures the sustainability of the synthesis of *N*-alkyl amines. Indeed, several efficient homogeneous catalytic reactions based on precious noble

metals^[6] as well as base-metal catalysts have been well developed for the BH reactions.^[7a]

However, the requirement of an extensive ligand synthesis, sensitivity, handling under practical conditions, and poor recovery of the catalysts are potential disadvantages. Providing earth-abundant base metal catalysts as an alternative to precious noble metal catalysts represents a key challenge in contemporary science.^[7] Similarly, alternative benign approaches to employing stoichiometric reagents in industrially important reactions are vital. In this direction, the prime research objective of the chemical and pharmaceutical industries is to convert homogeneous catalytic reactions into heterogeneous versions through the immobilization of catalytically active sites on stable supports.^[8] Heterogeneous catalysts have numerous advantages over homogeneous ones, including high recyclability and easy recovery from the reaction mixture.

Various heterogeneous cobalt,^[9] nickel,^[10] and iron-based catalysts^[11] have made a substantial contribution to the field of dehydrogenation and related reactions. Notably, the employment of the manganese-based catalytic system, the third most abundant metal in the earth's crust, found manifold applications in synthetic transformation.^[12] In recent years, remarkable progress in homogeneous Mn-catalyzed acceptorless dehydrogenation (AD) and BH reactions has been made by several research groups including Milstein, Beller, Kirchner, Sortais, Kempe, and others (Scheme 1).^[7,13] However, a reusable heterogeneous manganese-based catalyst system for the BH strategy remains elusive. Particularly, the *N*-alkylation of amines under the BH strategy using heterogeneous catalyzed conditions is very limited and rarely reported.^[10,14]

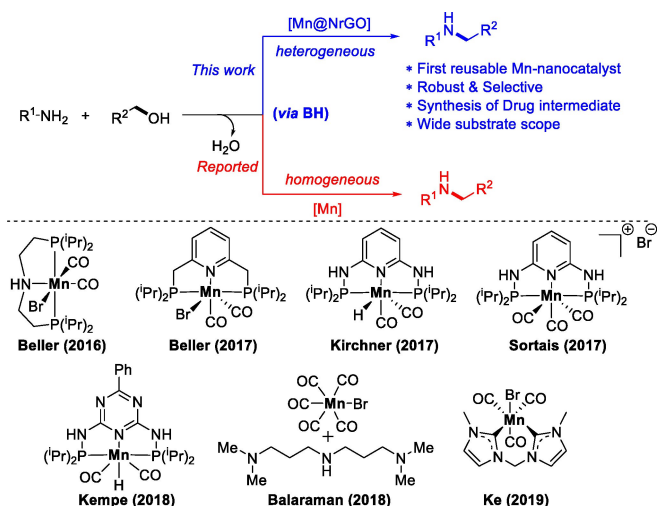
Of late, a variety of noble-metal nanoparticles decorated on an electron-rich carbon, which delivers active sites for the catalyst, have been widely investigated. Sustainable development of the heteroatom-doped carbon-based supports is fascinating due to their semiconductive nature, in which electronic density can be tuned by the amount of heteroatom doping. Due to the presence of lone pairs, the heteroatom

[a] M. Subaramanian, P. M. Ramar, G. Sivakumar, Prof. E. Balaraman
Department of Chemistry
Indian Institute of Science Education and Research (IISER) Tirupati
517507, Tirupati (India)
E-mail: eb.raman@iisertirupati.ac.in

[b] Dr. R. G. Kadam, Dr. M. Petr, Prof. R. Zboril, Prof. M. B. Gawande
Regional Centre of Advanced Technologies and Materials
Palacky University
78371, Olomouc (Czech Republic)

Supporting information for this article is available on the WWW under <https://doi.org/10.1002/cctc.202100635>

This publication is part of a Special Collection on "Supported Nanoparticles and Single-Atoms for Catalysis: Energy and Environmental Applications". Please check the ChemCatChem homepage for more articles in the collection.



Scheme 1. Recently reported homogeneous manganese-based catalysts for *N*-alkylation reactions *via* borrowing hydrogen vs our approach using a heterogeneous manganese nanocatalyst.

provides additional electrons in the π -conjugated system, which increases the charge density on the carbon sheets.^[15] It is also believed that the synergism between the individual counterparts (metal or support) often contributes to their superior catalytic performance.

In recent years, *N*-doped carbon-supported metal-based catalysts found widespread applications in sustainable chemical synthesis.^[11,16] Very recently, Karak and co-workers reported the reduced graphene oxide (rGO) based bi-phasic crystal of MnO_2 containing heterostructured hybrid nanoflower for *N*-alkylation reactions under aerobic conditions.^[16] The use of oxygen-rich rGO@ α - MnO_2 /rGO@ δ - MnO_2 catalyst facilitates the oxidation of alcohol to generate aldehyde and further condensation of amines with an aldehyde followed by the production of amines was observed under aerobic, solvent-free conditions. Importantly, the reaction system failed to evidence the borrowing hydrogen mechanism (*i.e.*, acceptorless dehydrogenation and re-hydrogenation pathway). Herein, we report a thermal decomposition of an *in situ* formed manganese complex on carbon support to procure robust, reusable nitrogen-doped graphene supported Mn-nanocatalyst (Mn@NrGO) for borrowing hydrogen reaction under anaerobic conditions. The synthesized catalyst demonstrates excellent activity and selectivity for the *N*-alkylation of amines using alcohol as the alkylating agent under mild, benign conditions. Notably, the manganese-based reusable heterogeneous catalysts for the BH reaction have remained elusive.

Results and discussion

Catalyst Preparation and Characterization

The active heterogeneous Mn@NrGO catalyst for the *N*-alkylation reaction was synthesized based on our previously

reported procedure.^[11c,d] Firstly, the *in situ* generated Mn-Phen complex ($\text{Mn}(\text{acac})_3$; 1,10-phenanthroline = 1:1) was deposited on an exfoliated graphene oxide support (rGO) and heated at 800 °C for 4 h under argon atmosphere. The obtained catalytic material represented as Mn@NrGO was characterized using PXRD, TEM, HRTEM-elemental mapping analysis, XPS, and ICP analysis.

In the powder X-ray diffraction (PXRD) spectrum of Mn@NrGO , the broad diffraction peak at 30.9° with the interplanar *d*-spacing of 0.33 nm, ascribed to the existence of nitrogen-doped graphitic carbon with hexagonal space group P63/mmc (PDF card 04-007-2081). The peaks at (2 θ) 40.84°, 47.52°, and 69.46° with the *d*-spacing of 0.256, 0.221, and 0.156 nm are equivalents to crystal planes of (111), (200) and (220), and characterize the MnO (space group Fm3m JCPDS card number 04-005-4473) (Figure S3, see ESI).

The X-ray photoelectron spectroscopy (XPS) was utilized to identify the surface properties and elemental composition of the catalyst (Figure 1). The Mn@NrGO catalyst exposed the co-existence of C, N, O, and Mn with 90.8, 1.9, 6.4, and 0.9%, respectively. The C 1s spectrum depicts the central contribution of the four peak components with binding energies of 284.82, 285.88, 286.77, and 287.87 eV related to C–C sp^3 , C–C sp^2 , C–O/C–N, and C=O or O=C–O type of carbons, which reveals the graphitic characteristics (Figure 1a). The N 1s spectrum can be resolved into two peaks at 398.89, and 401.81 eV, corresponding to the pyridinic, and pyrrolic nitrogen (Figure 1b). The O1s spectrum of Mn@NrGO (Figure 1c) can be classified into three-peak components with binding energies of 533.71, 531.77, and 530.30 eV, which confirm the presence of C–O, C=O and Mn–O, respectively; the oxygen on the surface of manganese proves that the graphitic carbon is doped with oxygen. The two-component peaks having their binding energies at 642.08 (Mn2p_{3/2}) and 646.08 eV (Mn2p_{1/2}) confirm the occurrence of manganese with +4 oxidation state (Figure 1d).^[17]

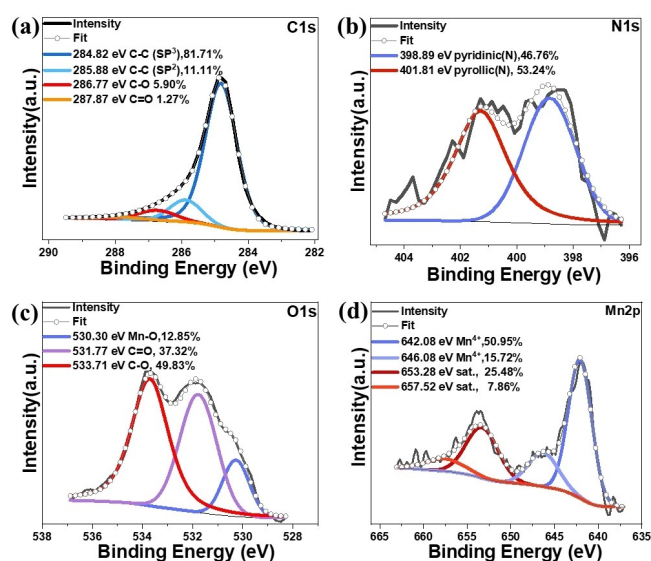


Figure 1. High resolution XPS spectra of Mn@NrGO catalyst (a) C1s, (b) N1s, (c) O1s, and (d) Mn2p region.

In Raman spectrum (Figure S3), the G band around 1600 cm^{-1} further confirms the presence of graphitic carbon. The band near 648 cm^{-1} is observed because of the existence of symmetric stretching vibration of Mn–O (Figure S4, see ESI). The TEM images (Figures 2a–b) display the distribution of the spherical shaped MnO_2 nanoparticles (30–60 nm) throughout the surface of *N*-doped-rGO. The 0.48 nm lattice spacing of the MnO_2 particles is observed with HRTEM (Figure 2c).^[17] Furthermore, a representative high-angle annular dark-field scanning (HAADF-STEM) image (Figure 2d) and the elemental mapping support the presence of C, N, O, and Mn mapping with the

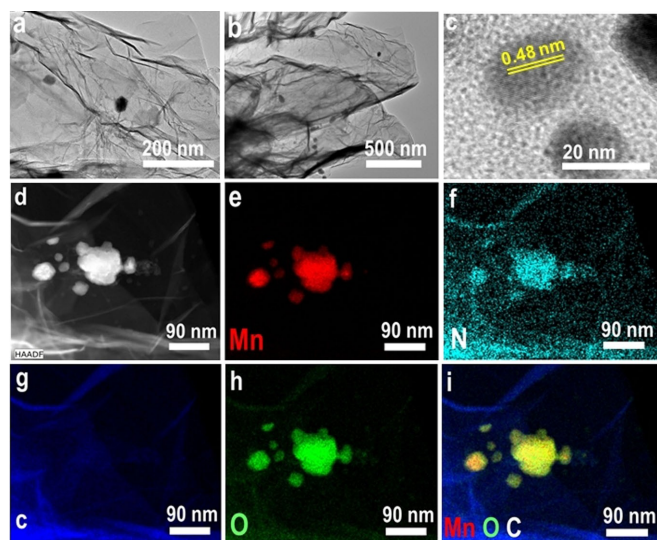


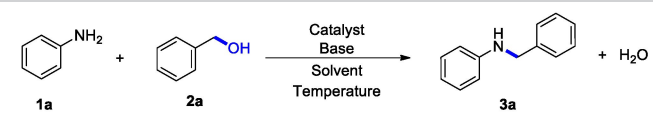
Figure 2. TEM images of Mn@NrGO (a and b), HRTEM image (c). HAADF-STEM image (e–i) elemental mapping showing Mn, N, C, O and Mn, O and C together.

consistent distribution of MnO_2 nanoparticles (Figure 2e–i). The well-characterized Mn@NrGO catalysts were further investigated, using alcohols as alkylating agents, for the direct and selective *N*-alkylation of amines. Initially, we began our exploration using aniline **1a** and benzyl alcohol **2a** as benchmark substrates for the optimization of ideal reaction conditions (Table 1).

The reactions of **1a** and **2a** in the presence of a catalytic amount of Mn@NrGO and KO^tBu (1 equiv.) in *n*-octane heated at 140°C (oil-bath temperature) under argon atm for 24 h gave the desired *N*-alkylated amine **3a** in 89% of isolated yield (Table 1, Entry 1). Moreover, the temperature plays an important role in this transformation, and it was noted that its lowering causes a decrease in the product formation (Table 1, Entries 2–3). The solvent screening for the *N*-alkylation of **1a** was carried out using various solvents such as *n*-octane, toluene, 1,4 dioxane, and THF (Table 1, entries 1 and 8–10), and it was found that *n*-octane was an appropriate solvent for an effective *N*-alkylation reaction. Prominently, a decrease in the amount of the catalyst loading afforded a lower yield of **3a** (Table 1, Entries 4–5). In addition, decreasing the amount of base (KO^tBu) resulted in the 71% yield of **3a** (Table 1, Entry 6); in the absence of base, no product formation was observed (Table 1, Entry 11). However, the efficiency of the reaction was significantly affected in the presence of other bases like NaO^tBu, Na_2CO_3 , K_2CO_3 , and KOH (Table 1, Entries 12–15). In the absence of Mn@NrGO, the reaction afforded only 18% yield of **3a** (Table 1, Entry 16). Notably, the reaction failed to yield the product or hydrogen gas under homogeneous conditions (Table 1, Entry 17).

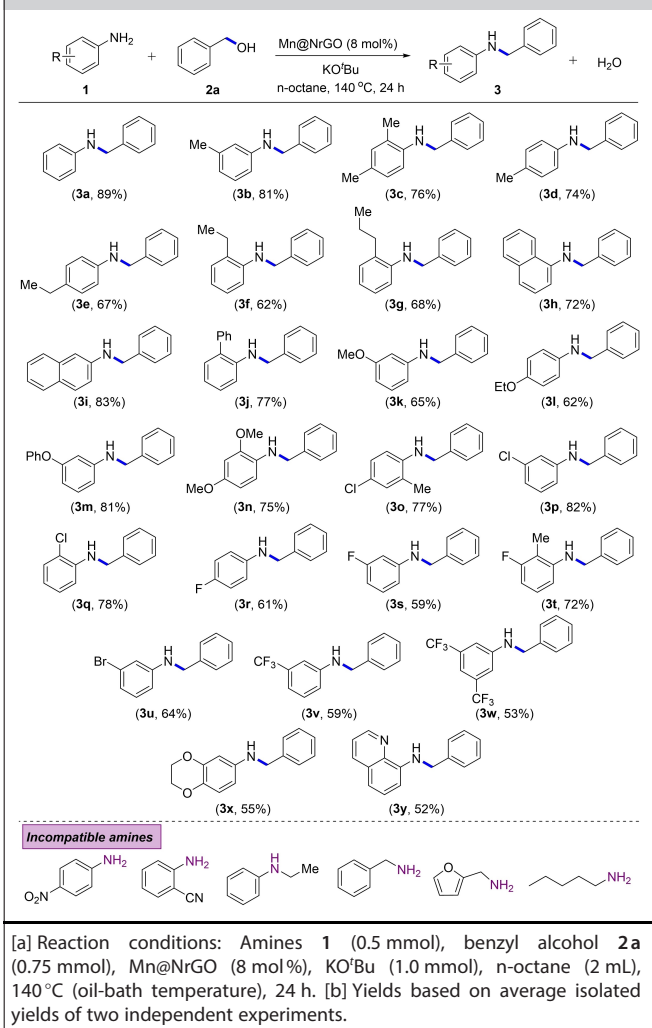
Having optimized the reaction conditions, we explored a variety of amines in the *N*-alkylation reaction using benzyl alcohol (**2a**) (Table 2). It should be pointed out that the

Table 1. Optimization of reaction conditions for *N*-alkylation of aniline with benzyl alcohol.^[a]



Entry	Catalyst [mol%]	Base [equiv.]	Solvent	T [°C]	t [h]	Yield [%] ^[b]
1	Mn@NrGO (8)	KO ^t Bu (1)	<i>n</i> -Octane	140	24	89
2	Mn@NrGO (8)	KO ^t Bu (1)	<i>n</i> -Octane	100	24	59
3	Mn@NrGO (8)	KO ^t Bu (1)	<i>n</i> -Octane	80	24	42
4	Mn@NrGO (5)	KO ^t Bu (1)	<i>n</i> -Octane	140	24	76
5	Mn@NrGO (2.5)	KO ^t Bu (1)	<i>n</i> -Octane	140	24	65
6	Mn@NrGO (8)	KO ^t Bu (0.5)	<i>n</i> -Octane	140	24	71
7	Mn@NrGO (8)	KO ^t Bu (1)	<i>n</i> -Octane	140	12	81
8	Mn@NrGO (8)	KO ^t Bu (1)	Toluene	140	24	57
9	Mn@NrGO (8)	KO ^t Bu (1)	Dioxane	140	24	23
10	Mn@NrGO (8)	KO ^t Bu (1)	THF	140	24	n.r
11	Mn@NrGO (8)	–	<i>n</i> -Octane	140	24	n.r
12	Mn@NrGO (8)	NaO ^t Bu (1)	<i>n</i> -Octane	140	24	36
13	Mn@NrGO (8)	Na_2CO_3 (1)	<i>n</i> -Octane	140	24	14
14	Mn@NrGO (8)	K_2CO_3 (1)	<i>n</i> -Octane	140	24	27
15	Mn@NrGO (8)	KOH (1)	<i>n</i> -Octane	140	24	32
16	–	KO ^t Bu (1)	<i>n</i> -Octane	140	24	18
17 ^[c]	Mn(acac) ₃ + 1, 10-Phen (8)	KO ^t Bu (1)	<i>n</i> -Octane	140	24	trace

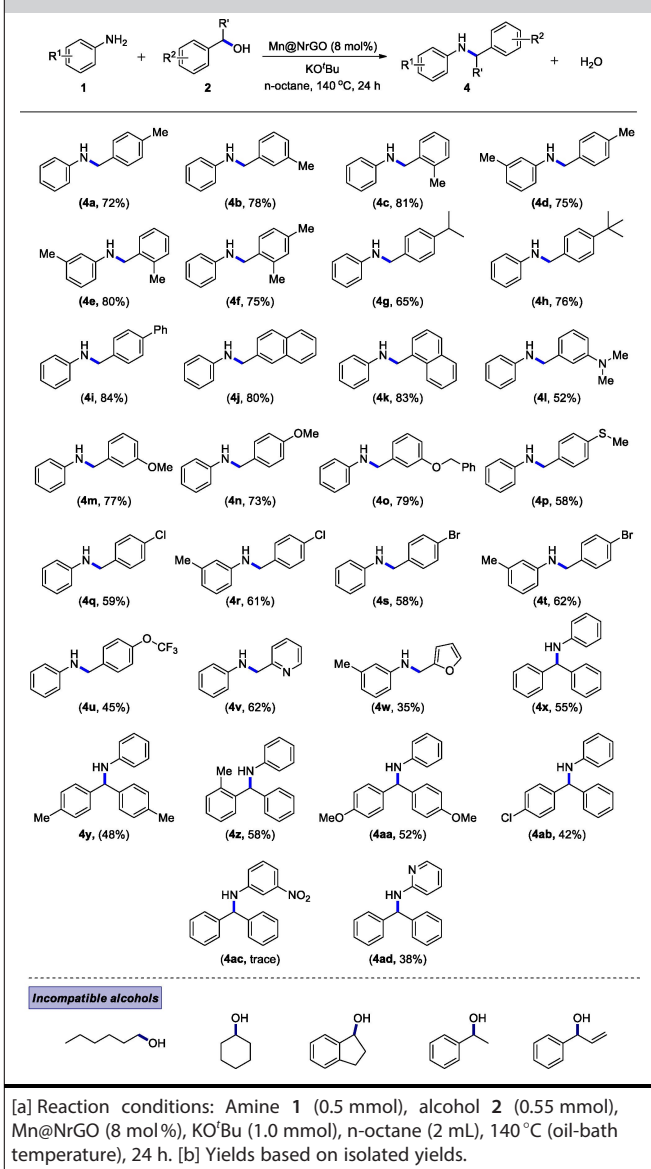
[a] Reaction conditions: Aniline **1a** (0.5 mmol), benzyl alcohol **2a** (0.75 mmol), catalyst (x mol%), base (y equiv.), solvent (2 mL), 140°C (oil-bath temperature), 12–24 h. [b] Isolated yields. [c] Under homogeneous conditions.

Table 2. Mn@NrGO catalyzed *N*-alkylation of amines with benzyl alcohol: Scope of amines.^[a,b]


Mn@NrGO nanocatalyst was compatible with various anilines comprising electron-rich substituents at *ortho*, *meta*, *para*-positions and produced the corresponding secondary amine derivatives (**3a–3g**) in good to excellent yields under mild and benign conditions. Importantly, a fused aromatic hydrocarbon containing amines such as 1-naphthalamine and 2-naphthalamine afforded the corresponding *N*-alkylated products **3h** in 72% and **3i** in 83% of isolated yields, respectively. Aniline derivatives containing strong electron-rich substituents (-Ph, -OMe, -OPh, and -OEt) led to the desired products **3j–3n** in good to excellent yields (62–81%). Besides, halide substituted aromatic amines (-F, -Cl, and -Br) yielded the desired *N*-alkylated product smoothly under heterogeneous Mn-catalyzed conditions (products **3o–3u** in 59–82% yields). Particularly, pharmaceutically active 3-trifluoro-, 1,3-trifluoro-, and 1,4-dioxalane substituted anilines derivatives underwent *N*-alkylation reaction and resulted in the corresponding secondary amine products **3v** in 59%, **3w** in 53%, and **3x** in 55% yields, respectively. Interestingly, heterocyclic 8-aminoquinoline gave a 52% yield of the *N*-alkylated product (**3y**). However, the aniline containing

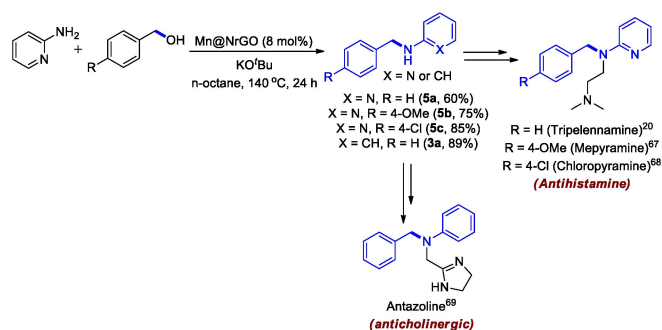
a strong electron-withdrawing group (-NO₂, -CN) afforded only a trace amount of the product and *N*-ethyl aniline did not yield the *N*-alkylated product under our reaction conditions. Moreover, benzylamine, furfurylamine, and aliphatic amine such as hexylamine are incompatible with the present Mn-catalyzed conditions.

We further examined the scope of alcohols for the selective *N*-alkylation of **1a** under heterogeneous Mn-catalyzed conditions (Table 3). The electron-releasing substituents (methyl, *isopropyl*, *t*-butyl, and phenyl) on the benzyl alcohol react with aniline **1a** or 3-methyl aniline (**1b**) to give the *N*-alkylated products **4a–4i** in 65–84% yields. Significantly, π -extended bicyclic alcohols such as 2-naphthalene methanol and 1-naphthalene methanol yielded the expected *N*-alkylated products **4j** in 80% and **4k** in 83% yields, respectively. In addition, strong electron-donating substituents (-OMe, -SMe, -NMe₂, and benzyloxy groups) on benzyl alcohols gave the desired

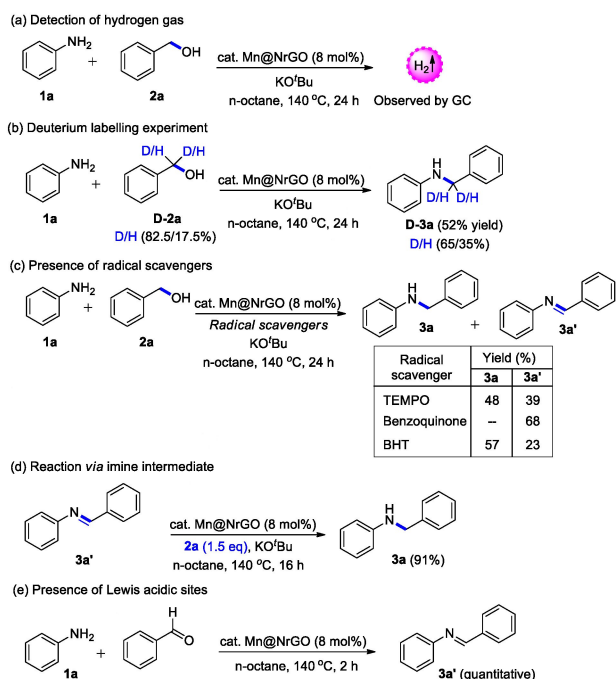
Table 3. Mn@NrGO catalyzed *N*-alkylation of amines with alcohols: Scope of alcohols.^[a,b]


products in moderate to good yields (products **4l–4p** in 52–79% yields). The substrates bearing halide substituent (-Cl, -Br) afforded the products **4q–4t** in 58–62% isolated yields, respectively. Trifluoromethylated ether containing benzyl alcohol gave product **4u** in 45% under the present heterogeneous Mn-based nanocatalyst conditions. Heteroaromatic alcohols such as pyridine 2-methanol (**2v**) and furfuryl alcohol (**2w**) gave desired products **4v** in 62% and **4w** in 35% yields, respectively, under optimized reaction conditions.

It should be noted that more steric secondary alcohols such as diphenylmethanol and diphenylmethanol bearing -Me, -OMe, and -Cl groups afforded the corresponding *N*-alkylated products **4x–4ab** in 42–58% of isolated yields. However, diphenylmethanol reacting with strong electron-withdrawing 3-nitro aniline did not yield the desired product (**4ac**) under our reaction conditions. Moreover, diphenylmethanol with 2-aminopyridine gave the expected product **4ad** in 38% of isolated



Scheme 2. Synthesis of pharmaceutically important *N*-alkylated amine intermediates catalyzed by Mn@NrGO.



Scheme 3. Mechanistic studies.

yields. Indeed, secondary alcohol such as 1-phenylethanol, 1-indanol, α -vinyl benzylalcohol, cyclohexanol, and aliphatic primary alcohol (1-hexanol) was incompatible under our heterogeneous Mn catalyzed conditions.

We effectively applied our catalytic system to the synthesis of antihistamine and anticholinergic drug intermediates (**5a–5c**).^[66,18] Thus, the pharmaceutically active intermediates **5a**, **5b**, and **5c** were prepared in good yields with excellent step- and atom-economy under our heterogeneous manganese catalytic conditions (Scheme 2).

To gain insight into the reaction mechanism, we have performed several control experiments (Scheme 3). The formation of hydrogen gas and the dehydrogenated product (aldehyde) was qualitatively observed in the initial dehydrogenation of alcohol (**2a**) under Mn-catalytic conditions in the absence of an amine coupling partner (see ESI). Similarly, the formation of hydrogen gas was also observed from the benchmark reaction (Scheme 3a). The deuterium labelling experiment using deuterated benzyl alcohol (**D-2a**) with aniline (**1a**) resulted in 65% of deuterium incorporation in the secondary amine (Scheme 3b). These results indicate that the reaction proceeds *via* the dehydrogenation of alcohol (**2a**). Next, to determine if any radical intermediates (e.g., superoxide radical anion, $\text{O}^{\bullet-2}$; due to the presence of residual oxygen/air or use of KO^tBu) were involved in the reaction, we performed the reaction in the presence of radical scavengers. Thus, the presence of various radical scavengers such as TEMPO, benzoquinone, and butylated hydroxytoluene (BHT) did not affect the reactivity of the catalyst and, thus, product **3a** and the corresponding imine intermediate (**3a'**) were produced in good yields (Scheme 3c). This result indicates that the radical pathway was not possible under our reaction conditions, and the reaction proceeded *via* an imine intermediate. Indeed, KO^tBu is required to activate alcohols for the initial dehydrogenation reaction. Next, treatment of imine (**3a'**) under the present heterogeneous Mn-nanocatalytic conditions using alcohol as the transfer hydrogenating source selectively yielded the desired *N*-alkylated amine (**3a**) (Scheme 3d). Finally, we have endeavored to investigate the effect of the Mn-nanocatalyst in the condensation step (imine formation). It was clearly observed that the rate of condensation of aldehyde and aniline was accelerated in the presence of the Mn-nanocatalyst, which implies the presence of Lewis acid sites on the catalyst. Overall, all these studies revealed that the reaction preceded *via* the borrowing hydrogenation.

The reaction kinetic profile was conducted for the reusable heterogeneous Mn-catalyzed *N*-alkylation of aniline (**1a**) with benzyl alcohol (**2a**) (Figure 3a). The time-dependent product formation clearly showed that the starting material aniline **1a** was completely consumed in 20 h and the *N*-alkylated product formation **3a** increased gradually with the increasing reaction time. Notably, no other intermediate was detected in the spectroscopic analysis.

The main advantage of heterogeneous catalysis is easy recovery and recyclability of the catalyst. The developed manganese-nanocatalyst retained its catalytic activity even after six consecutive reaction cycles and offered the *N*-alkylated

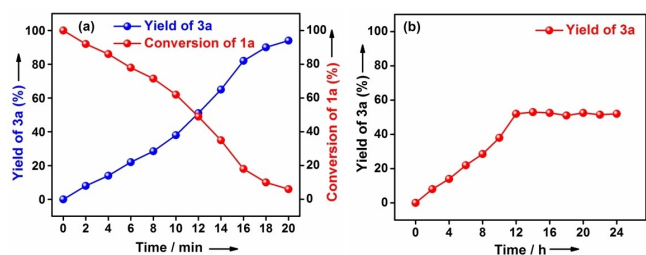


Figure 3. (a) Kinetic plot for the heterogeneous Mn-catalyzed *N*-alkylation of aniline and (b) Hot filtration test.

product **3a** in an excellent yield for the benchmark reaction (Figure 4). Interestingly, the recyclability test at the intermediate conversion level (45%) showed similar outcomes. This result suggests that the developed Mn-nanocatalyst is highly robust and does not undergo deactivation during the catalysis. XPS studies of spent Mn-catalyst revealed that there are no significant changes in the surface properties and elemental composition.

Further, to confirm the heterogeneity of the present Mn-nanocatalyst, a hot filtration test was conducted (Figure 3b). When the Mn-catalyst was removed from the reaction mixture after 12 h (52% yield of **3a**), no further increase in the product (**3a**) yield followed. Notably, a trace amount of product formation was observed under complete homogeneous reaction conditions (Table 1, Entry 18). These results clearly show that the present Mn-nanocatalyst is truly heterogeneous in nature.

Based on the above-mentioned experimental results, we confirm that the present heterogeneous manganese nanocatalyst catalyzed *N*-alkylation of amines using alcohols as alkylating agents follows the borrowing hydrogenation mechanism. Initially, in the presence of Mn@NrGO and base, the alcohol underwent a dehydrogenation reaction and yielded the dehydrogenative product aldehyde with the liberation of hydrogen gas. Subsequently, the condensation reaction of aldehyde with amine to form the intermediate imine with the liberation of water. Finally, the (transfer) hydrogenation of imine intermediate using hydrogen gas generated in the initial alcohol dehydrogenation step selectively offered the expected *N*-alkylated amine (Scheme 4).^[4d,7a] Consequently, the *N*-alkyla-

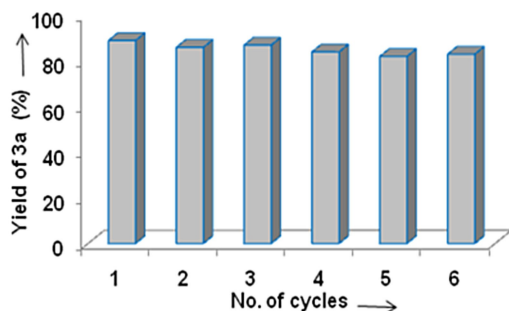
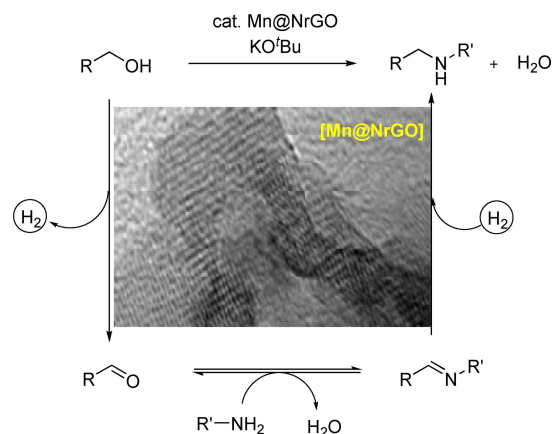


Figure 4. Recyclability test.



Scheme 4. A plausible reaction mechanism.

tion of anilines using alcohols as an alkylating agent *via* borrowing hydrogenation under heterogeneous Mn-catalyzed conditions has been achieved.

Conclusion

In conclusion, we have developed the nitrogen-doped graphene supported Mn-based nanocatalyst for *N*-alkylation of amines using alcohols as an alkylating agent under mild, benign conditions. The present *N*-alkylation reaction provides a simple and atom-economical route to various secondary amine derivatives with a wide substrate scope, as well as excellent functional group tolerance. Mechanistic studies and deuterium labelling studies revealed that the reaction proceeded *via* borrowing hydrogenation. Favorably, the manganese-nanocatalyst retains its catalytic activity even after six consecutive reaction cycles and offers the *N*-alkylated product in excellent yields.

Experimental Section

Catalyst Characterization

Powder X-ray diffraction (XRD) patterns of the material were inspected by the X'Pert PRO MPD diffractometer (PANalytical) in the Bragg-Brentano geometry with an iron-filtered X'Celerator detector and programmable divergence, and diffracted beam antiscatter-slits at room temperature using a Co-K α radiation (40 kV, 30 mA, $\lambda = 0.1789$ nm). The angular range of the measurement was set as $2\theta = 5-90^\circ$, with a step size of 0.017° . The identification of the crystalline phases in the experimental XRD pattern was obtained using the X'Pert High Score Plus software, which includes a PDF-4+ and ICSD databases. The SRM660 (LaB6) standard was used to evaluate the instrumental broadening. The X-ray diffraction lines were modelled using pseudo-Voigt functions, and a single-split asymmetry correction was introduced. Additional quantitative analysis and determination of the crystalline domain sizes were performed on the Mn@NrGO sample following the Rietveld method.

Microscopic TEM images were obtained by HRTEM TITAN 60–300 with the X-FEG type emission gun, operating at 80 kV. This microscope is equipped with a Cs image corrector and a STEM high-angle annular dark-field detector (HAADF). The point resolution is 0.06 nm in the TEM mode. The elemental mappings were obtained by the STEM-Energy Dispersive X-ray Spectroscopy (EDS) with an acquisition time of 20 min. For the HRTEM analysis, the powder samples were dispersed in ethanol and ultrasonicated for 5 min. One drop of this solution was placed on a copper grid with a holey carbon film.

The XPS surface investigation was performed on the PHI 5000 VersaProbe II XPS system (Physical Electronics) with a monochromatic Al-K α source (15 kV, 50 W) and photon energy of 1486.7 eV. Dual-beam charge compensation was used for all the measurements. All the spectra were measured in the vacuum of 1.3×10^{-7} Pa and at a room temperature of 21 °C. The analyzed area on each sample was a spot of 200 μ m in diameter. The survey spectra were measured at a pass energy of 187.850 eV and an electronvolt step of 0.8 eV. For the high-resolution spectra, pass energy of 23.500 eV and electronvolt step of 0.2 eV were used. The spectra were evaluated with the MultiPak (Ulvac - PHI, Inc.) software. All binding energy (BE) values were referenced to the carbon peak C1s at 284.80 eV.

General Procedure for the Heterogeneous Manganese-Catalyzed *N*-Alkylation of anilines

To an oven-dried 15 mL screw-capped reaction tube, amine 1 (0.5 mmol, 1 equiv.), alcohol 2 (0.75 mmol, 1.5 equiv.), Mn@NrGO catalyst (25 mg, 8 mol%), KO^tBu (0.5 mmol, 1 equiv.), and *n*-octane (2 mL) were added under a gentle stream of argon. The reaction mixture was continuously stirred at 140 °C for 24 h. After completion of the reaction, the crude mixture was diluted with ethyl acetate (3 \times 5 mL) and the catalyst was separated by centrifugation. The resultant supernatant liquid of organic layer was dried over anhydrous Na₂SO₄ and the solvent was evaporated under reduced pressure. The crude mixture was purified by silica gel column chromatography (230–400 mesh size) using petroleum-ether/ethyl acetate as an eluting system.

Acknowledgements

This research work was supported by IISER Tirupati, and SERB, India (Grant No: CRG/2018/002480/OC). EB acknowledges funding from SwarnaJayanti Fellowship (DST/SJF/CSA-04/2019–2020 and SERB/F/5892/2020–2021). MS thanks the UGC for the research fellowship. GS thanks IISER Tirupati for the research fellowship. The authors gratefully acknowledge the support by the Operational Program Research, Development and Education – European Regional Development Fund (CZ.02.1.01/0.0/0.0/16_019/0000754) and the Ministry of Education, Youth and Sports of the Czech Republic (CZ.02.1.01/0.0/0.0/17_048/0007323).

Conflict of Interest

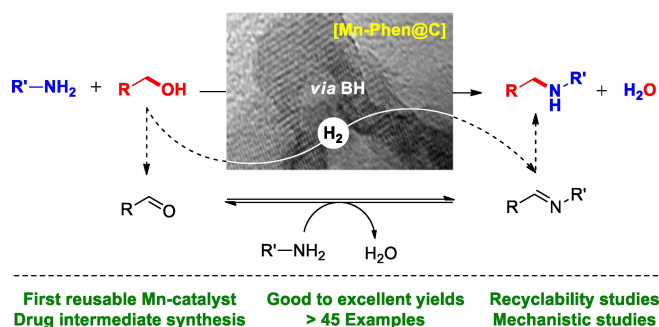
The authors declare no conflict of interest.

Keywords: Alcohols · Amination · Heterogeneous catalysis · Hydrogen · Manganese catalyst

- [1] a) S. A. Lawrence, *Amines: Synthesis Properties and Applications*, Cambridge University Press, Cambridge 2004; b) J. L. McGuire, *Pharmaceuticals: Classes, Therapeutic Agents, Areas of Application*, Wiley-VCH: Weinheim, Germany 2000, p 1–4. A. S. Travis, in *The Chemistry of Anilines Vol. 1* (ed. Rappoport, Z.) 717 (Wiley-Interscience, 2007); c) A. Ricci, *Amino Group Chemistry, From Synthesis to the Life Sciences*, Wiley-VCH, Weinheim 2007; d) T. C. Nugent, M. El-Shazly, *Adv. Synth. Catal.* 2010, 352, 753–819; e) E. Vitaku, D. T. Smith, J. T. Njardarson, *J. Med. Chem.* 2014, 57, 10257–10274.
- [2] a) J. F. Hartwig, *Acc. Chem. Res.* 1998, 31, 852–860; b) M. B. Smith, J. March, *March's Advanced Organic Chemistry: Reactions, Mechanisms, and Structure*, John Wiley & Sons 2007.
- [3] S. Raoufoghaddam, *Org. Biomol. Chem.* 2014, 12, 7179–7193.
- [4] a) G. Guillena, D. J. Ramón, M. Yus, *Chem. Rev.* 2010, 110, 1611–1641; b) M. H. S. A. Hamid, P. A. Slatford, J. M. J. Williams, *Adv. Synth. Catal.* 2007, 349, 1555–1575; c) Q. Yang, Q. Wang, Z. Yu, *Chem. Soc. Rev.* 2015, 44, 2305–2329; d) C. Gunanathan, D. Milstein, *Science* 2013, 341, 249–260; e) A. Corma, J. Navas, M. J. Sabater, *Chem. Rev.* 2018, 118, 1410–1459.
- [5] J. Magano, J. R. Dunetz, *Chem. Rev.* 2011, 111, 2177–2250.
- [6] a) A. Bartoszewicz, R. Marcos, S. Sahoo, K. N. Inge, X. Zou, B. Martín-Matute, *Chem. Eur. J.* 2012, 18, 14510–14519; b) K.-i. Fujita, Y. Enoki, R. Yamaguchi, *Tetrahedron* 2008, 64, 1943–1954; c) Z. Zhu, J. H. Espenson, *J. Org. Chem.* 1996, 61, 324–328; d) J.-Q. Li, P. G. Andersson, *Chem. Commun.* 2013, 49, 6131–6133; e) Q. Zou, C. Wang, J. Smith, D. Xue, J. Xiao, *Chem. Eur. J.* 2015, 21, 9656–9661; f) M. H. S. A. Hamid, C. L. Allen, G. W. Lamb, A. C. Maxwell, H. C. Maytum, A. J. A. Watson, J. M. J. Williams, *J. Am. Chem. Soc.* 2009, 131, 1766–1774; g) K. O. Marichev, J. M. Takacs, *ACS Catal.* 2016, 6, 2205–2210; h) T. T. Dang, B. Ramalingam, S. P. Shan, A. M. Seayad, *ACS Catal.* 2013, 3, 2536–2540.
- [7] a) T. Irrgang, R. Kempe, *Chem. Rev.* 2019, 119, 2524–2549; b) A. Mukherjee, D. Milstein, *ACS Catal.* 2018, 8, 11435–11469.
- [8] a) L. Liu, A. Corma, *Chem. Rev.* 2018, 118, 4981–5079; b) R. K. Sharma, S. Dutta, S. Sharma, R. Zbořil, R. S. Varma, M. B. Gawande, *Green Chem.* 2016, 18, 3184–3209; c) D. Nandan, G. Zoppellaro, I. Medřik, C. Aparicio, P. Kumar, M. Petr, O. Tomanec, M. B. Gawande, R. S. Varma, R. Zbořil, *Green Chem.* 2018, 20, 3542–3556.
- [9] a) R. V. Jagadeesh, K. Murugesan, A. S. Alshammari, H. Neumann, M. M. Pohl, J. Radnik, M. Beller, *Science* 2017, 358, 326–332; b) T. Senthamarai, V. G. Chandrashekhar, M. B. Gawande, N. V. Kalevaru, R. Zbořil, P. C. J. Kamer, R. V. Jagadeesh, M. Beller, *Chem. Sci.* 2020, 11, 2973–2981.
- [10] K.-i. Shimizu, N. Imaiida, K. Kon, S. M. A. H. Siddiki, A. Satsuma, *ACS Catal.* 2013, 3, 998–1005.
- [11] a) R. V. Jagadeesh, A.-E. Surkus, H. Junge, M.-M. Pohl, J. R. Radnik, J. Rabeah, H. Huan, V. Schunemann, A. Bruckner, M. Beller, *Science* 2013, 342, 1073–1076; b) M. B. Gawande, P. S. Branco, R. S. Varma, *Chem. Soc. Rev.* 2013, 42, 3371–3393; c) G. Jaiswal, V. G. Landge, D. Jagadeesan, E. Balaraman, *Nat. Commun.* 2017, 8, 2147–2159; d) G. Jaiswal, V. G. Landge, D. Jagadeesan, E. Balaraman, *Green Chem.* 2016, 18, 3232–3238.
- [12] a) W. Liu, J. T. Groves, *Acc. Chem. Res.* 2015, 48, 1727–1735; b) A. Gunay, K. H. Theopold, *Chem. Rev.* 2010, 110, 1060–1081.
- [13] a) S. Elangovan, J. Neumann, J.-B. Sortais, K. Junge, C. Darcel, M. Beller, *Nat. Commun.* 2016, 7, 12641–12648; b) R. Fertig, T. Irrgang, F. Freitag, J. Zander, R. Kempe, *ACS Catal.* 2018, 8, 8525–8530; c) V. G. Landge, A. Mondal, V. Kumar, A. Nandakumar, E. Balaraman, *Org. Biomol. Chem.* 2018, 16, 8175–8180; d) M. Huang, Y. Li, Y. Li, J. Liu, S. Shu, Y. Liu, Z. Ke, *Chem. Commun.* 2019, 55, 6213–6216; e) J. Neumann, S. Elangovan, A. Spannenberg, K. Junge, M. Beller, *Chem. Eur. J.* 2017, 23, 5410–5413; f) A. Bruneau-Voisine, D. Wang, V. Dorcet, T. Roisnel, C. Darcel, J.-B. Sortais, *J. Catal.* 2017, 347, 57–62; g) M. Mastalir, E. Pittenauer, G. Allmaier, K. Kirchner, *J. Am. Chem. Soc.* 2017, 139, 8812–8815; h) U. K. Das, Y. Ben-David, Y. Diskin-Posner, D. Milstein, *Angew. Chem. Int. Ed.* 2018, 57, 2179–2182; *Angew. Chem.* 2018, 130, 2201–2204.
- [14] a) K. Motokura, N. Nakagiri, T. Mizugaki, K. Ebitani, K. Kaneda, *J. Org. Chem.* 2007, 72, 6006–6015; b) K. Shimizu, M. Nishimura, A. Satsuma, *ChemCatChem* 2009, 1, 497–503; c) L. He, X.-B. Lou, J. Ni, Y.-M. Liu, Y. Cao, H.-Y. He, K.-N. Fan, *Chem. Eur. J.* 2010, 16, 13965–13969; d) W. He, L. Wang, C. Sun, K. Wu, S. He, J. Chen, P. Wu, Z. Yu, *Chem. Eur. J.* 2011, 17, 13308–13317; e) X. Cui, X. Dai, Y. Deng, F. Shi, *Chem. Eur. J.* 2013, 19, 3665–3675; f) M. M. Reddy, M. A. Kumar, P. Swamy, M. Naresh, K.

- Srujana, L. Satyanarayana, A. Venugopala, N. Narender, *Green Chem.* **2013**, *15*, 3474–3483; g) S. P. Pathare, K. G. Akamanchi, *Appl. Catal. A* **2013**, *452*, 29–33; h) P. Srinivasu, D. Venkanna, M. L. Kantam, J. Tang, S. K. Bhargava, A. Aldalbahi, K. C.-W. Wu, Y. Yamauchi, *ChemCatChem* **2015**, *7*, 747–751; i) A. Bayat, M. Shakourian-Fard, P. Nouri, M. M. Hashemi, *Appl. Organomet. Chem.* **2017**, *31*, 3720; j) F. Santoro, R. Psaro, N. Ravasio, F. Zaccheria, *RSC Adv.* **2014**, *4*, 2596–2600.
- [15] a) T. Cheng, H. Yu, F. Peng, H. Wang, B. Zhang, D. Su, *Catal. Sci. Technol.* **2016**, *6*, 1007–1015; b) M. Li, F. Xu, H. Li, Y. Wang, *Catal. Sci. Technol.* **2016**, *6*, 3670–3693; c) H. Wang, T. Maiyalagan, X. Wang, *ACS Catal.* **2012**, *2*, 781–794; d) L. He, F. Weniger, H. Neumann, M. Beller, *Angew. Chem. Int. Ed.* **2016**, *55*, 12582–12594; *Angew. Chem.* **2016**, *128*, 12770–12783.
- [16] a) M. B. Gawande, P. Fornasiero, R. Zbořil, *ACS Catal.* **2020**, *10*, 2231–2259; b) Z. Wei, Y. Chen, J. Wang, D. Su, M. Tang, S. Mao, Y. Wang, *ACS Catal.* **2016**, *6*, 5816–5822; c) W. Zhong, H. Liu, C. Bai, S. Liao, Y. Li, *ACS Catal.* **2015**, *5*, 1850–1856; d) K. Shen, L. Chen, J. Long, W. Zhong, Y. Li, *ACS Catal.* **2015**, *5*, 5264–5271; e) Y. Wang, Y. Nie, W. Ding, S. G. Chen, K. Xiong, X. Q. Qi, Y. Zhang, J. Wang, Z. D. Wei, *Chem. Commun.* **2015**, *51*, 8942–8945; f) A. Maleki, N. Ghamari, M. Kamalzare, *RSC Adv.* **2014**, *4*, 9416–9423; g) X. Dai, Z. Li, Y. Ma, M. Liu, K. Du, H. Su, H. Zhuo, L. Yu, H. Sun, X. Zhang, *ACS Appl. Mater. Interfaces* **2016**, *8*, 6439–6448; h) R. V. Jagadeesh, H. Junge, M.-M. Pohl, J. Radnik, A. Brückner, M. Beller, *J. Am. Chem. Soc.* **2013**, *135*, 10776–10782; i) H. Chaudhuri, N. Karak, *ChemCatChem* **2020**, *12*, 1617–1629.
- [17] W. Li, X. Cui, R. Zeng, G. Du, Z. Sun, R. Zheng, S. P. Ringer, S. X. Dou, *Sci. Rep.* **2015**, *5*, 8987.
- [18] A. Mehta, A. Thaker, V. Londhe, S. R. Nandan, *Appl. Catal. A* **2014**, *478*, 241–251.

Manuscript received: May 1, 2021
Revised manuscript received: July 27, 2021
Version of record online: ■■■, ■■■■



M. Subaramanian, P. M. Ramar, G. Sivakumar, Dr. R. G. Kadam, Dr. M. Petr, Prof. R. Zboril, Prof. M. B. Gawande, Prof. E. Balaraman*

1 – 9

Convenient and Reusable Manganese-Based Nanocatalyst for Amination of Alcohols



Nanocatalytic Amination: Herein, a reusable heterogeneous *N*-doped graphene-based manganese nanocatalyst (Mn@NrGO) for selective *N*-alkylation of amines with alcohols is described. The heterogeneous nature

of the catalyst made it easy to separate for long-term performance, and the recycling study revealed that the catalyst was robust and retained its activity after several recycling experiments.